

Difference analysis of shale gas-bearing property --A case study of the shale within Lower Cambrian Niutitang Formation on the margin of palaeouplift

Mingna Ge^{1*}, Shujing Bao¹, Yufang Wang¹, Haohan Li¹, Ting Wang¹, Hongbo Liang²

¹Oil and Gas Survey, China Geological Survey, China, ²Research Institute of Petroleum Exploration and Development (RIPED), China

Submitted to Journal:
Frontiers in Earth Science

Specialty Section:
Sedimentology, Stratigraphy and Diagenesis

Article type:
Original Research Article

Manuscript ID:
1447949

Received on:
12 Jun 2024

Revised on:
07 Dec 2024

Journal website link:
www.frontiersin.org

In review

Scope Statement

Study on geological conditions, main controlling factors of gas bearing and enrichment regularity of Cambrian shale gas in southern China

Conflict of interest statement

The authors declare that the research was conducted in the absence of any commercial or financial relationships that could be construed as a potential conflict of interest

Credit Author Statement

Yufang Wang: Writing - review & editing. Ting Wang: Writing - review & editing. Haohan Li: Writing - review & editing. Hongbo Liang: Writing - review & editing. Shujing Bao: Writing - review & editing. Mingna Ge: Conceptualization, Data curation, Formal Analysis, Investigation, Methodology, Writing - original draft, Writing - review & editing.

Keywords

Gas-bearing, Periphery of palaeouplift, shale gas, Niutitang Formation, Lower Cambrian

Abstract

Word count: 350

As a kind of high-quality clean energy and national strategic mineral resources, shale gas has developed rapidly in recent years and has become an important field for increasing oil and gas storage and production in China. However, it is mainly concentrated in the Marine Wufeng-Longmaxi shale Formation in Sichuan Basin. On the basis of the study of reservoir control model of early paleouplift, the characteristics of sedimentary facies, structural preservation, shale distribution, organic geochemistry, mineral association, reservoir physical property and gas-bearing are studied by taking the typical wells of Hannan palaeouplift, Shennongjia palaeouplift, Huangling palaeouplift and Xuefengshan palaeouplift in the periphery of Sichuan Basin. The organic matter type of the 7 wells in the study area is mainly type I, the average organic carbon content is 1.5% -3.56%, the average Ro is 2.37% -3.9%, the brittle minerals are mainly quartz, the content of quartz is 28% -53%, and the average porosity is 0.51% -3.34%. The pores contain organic pores, inorganic pores and micro-fractures, and the fractures are mostly -2 -filled with calcite. Gas content 0.13m³ /t -4.19m³ /t. Through comparative analysis of main controlling factors affecting gas content of shale, the causes of gas diversity of Niutitang Formation shale on the periphery of palaeouplift are identified. The results show that: (1) The differences in preservation conditions caused by structural strength, fracture development degree and the coupling relationship with tectonic fractures are the key factors restricting the gas content of shale; (2) The difference of thermal evolution degree caused by early deep burial time, long deep burial time and fast deep burial is the key factor restricting the gas content of shale; (3) The difference of hydrocarbon generation potential caused by sedimentary subfacies in the same facies zone is an important factor restricting the gas-bearing capacity of shale; (4) There are good geological conditions for the generation of shale gas in the periphery of palaeouplift, and the areas with good preservation conditions such as the lower Plate of thrust nappe, the degree of thermal evolution is less than 3.0%, and the deepwater facies of trough are favorable directions for further exploration.

Funding information

The National Natural Science Foundation of China (42130803) and the Geological Survey Project (DD20230257).

Funding statement

The author(s) declare that financial support was received for the research, authorship, and/or publication of this article.

Ethics statements

Studies involving animal subjects

Generated Statement: No animal studies are presented in this manuscript.

Studies involving human subjects

Generated Statement: No human studies are presented in the manuscript.

Inclusion of identifiable human data

Generated Statement: No potentially identifiable images or data are presented in this study.

In review

Data availability statement

Generated Statement: The original contributions presented in the study are included in the article/supplementary material, further inquiries can be directed to the corresponding author/s.

In review

Difference analysis of shale gas-bearing property

——A case study of the shale within Lower Cambrian

Niutitang Formation on the margin of palaeouplift

Mingna Ge,^{a,b*}, Shujing Bao^a, Yufang Wang^a, Haohan Li^a, Ting Wang^a, Hongbo Liang^c

^a, China University of Geosciences, Beijing 100083, China

^b, Oil and Gas Survey, China Geological Survey, Beijing 100083, China

^c, PetroChina Research Institute of Petroleum Exploration & Development, Beijing 100083,

China

*Corresponding author; Tel.: +86-10-64998647, E-Mail: 610144368@qq.com

Abstract: As a kind of high-quality clean energy and national strategic mineral resources, shale gas has developed rapidly in recent years and has become an important field for increasing oil and gas storage and production in China. However, it is mainly concentrated in the Marine Wufeng-Longmaxi shale Formation in Sichuan Basin. On the basis of the study of reservoir control model of early paleouplift, the characteristics of sedimentary facies, structural preservation, shale distribution, organic geochemistry, mineral association, reservoir physical property and gas-bearing are studied by taking the typical wells of Hannan palaeouplift, Shennongjia palaeouplift, Huangling palaeouplift and Xuefengshan palaeouplift in the periphery of Sichuan Basin. The organic matter type of the 7 wells in the study area is mainly type I, the average organic carbon content is 1.5% - 3.56%, the average Ro is 2.37% - 3.9%, the brittle minerals are mainly quartz, the content of quartz is 28% - 53%, and the average porosity is 0.51% - 3.34%. The pores contain organic pores, inorganic pores and micro-fractures, and the fractures are mostly

23 filled with calcite. Gas content $0.13\text{m}^3/\text{t}$ - $4.19\text{m}^3/\text{t}$. Through comparative analysis of main
24 controlling factors affecting gas content of shale, the causes of gas diversity of Niutitang
25 Formation shale on the periphery of palaeouplift are identified. The results show that: (1) The
26 differences in preservation conditions caused by structural strength, fracture development degree
27 and the coupling relationship with tectonic fractures are the key factors restricting the gas content
28 of shale; (2) The difference of thermal evolution degree caused by early deep burial time, long
29 deep burial time and fast deep burial is the key factor restricting the gas content of shale; (3) The
30 difference of hydrocarbon generation potential caused by sedimentary subfacies in the same facies
31 zone is an important factor restricting the gas-bearing capacity of shale; (4) There are good
32 geological conditions for the generation of shale gas in the periphery of palaeouplift, and the areas
33 with good preservation conditions such as the lower Plate of thrust nappe, the degree of thermal
34 evolution is less than 3.0%, and the deepwater facies of trough are favorable directions for further
35 exploration.

36
37 **Keywords:** Gas- bearing; Periphery of palaeouplift; Shale gas; Niutitang Formation; Lower
38 Cambrian

40 1. Introduction

41 The shale gas revolution in the United States has made the United States the
42 largest natural gas producer in the world (HAMMES et al., 2012). Commercial
43 production of major shale gas reservoirs from Barnett to Marcellus (Abouelresh et al.,
44 2012; Bruner et al., 2015), successfully reversed the situation of US natural gas

45 imports to exports, while changing the world's energy market land-scape. China's
46 shale gas has experienced nearly 20 years of exploration and has entered the
47 substantial commercial development stage. In 2013, China's shale gas production was
48 only 200 million cubic meters, and with the progress of exploration and development
49 theory and technology, Shale gas production has achieved rapid growth. In 2018, the
50 production exceeded 10 billion cubic meters, and in 2020, it exceeded 20 billion cubic
51 meters, with a 15% - 40% increase in production, and its growth gas source was
52 mainly concentrated in the Wufeng-Longmaxi Formation, Sichuan Basin (He et al.,
53 2016). The cumulative proved geological reserves have exceeded 2 trillion square
54 meters, and the cumulative shale gas production has exceeded 70 billion square
55 meters. However, China's shale gas production in 2022 is 24 billion cubic meters, up
56 4.3% year-on-year, slowing down compared with previous years. China's external
57 dependence on natural gas is still at a high level of 40%. In the background of energy
58 security ~~and carbon peak~~ and carbon neutrality, it is urgent to increase the exploration
59 and development of shale gas in new areas, new layers, new types and new fields (He
60 et al., 2021). Previous studies have shown that the periphery of palaeouplift has low
61 thermal evolution and relatively stable structural characteristics, which is an important
62 target area for the investigation of Cambrian shale gas in southern China, and
63 important discoveries have been made in many areas of the periphery of Palaeouplift.
64 The Well EYY1HF in Huangling Uplift, western Hubei Province has a daily gas
65 output of 78,300 m³ and an open flow rate of 28.84×10⁴ m³ (Bao et al., 2018), the
66 daily gas of Well Eyiye 1 was 6.02×10⁴ m³ with an open flow rate of 12.38×10⁴ m³

67 (Li et al., 2019; Zhang et al., 2020), Well SNY1 in Hannan Uplift has a stable
68 production flow of $21 \times 10^4 \text{ m}^3 / \text{day}$, all of which obtain high production shale gas,
69 achieving a major breakthrough in low-pressure shale gas reservoir. However, Well
70 GDD1, HY1 and HD 1 in Xuefeng Uplift, Well EHD1 in Shenlongjia Palaeouplift and
71 Well SNY1 in Hannan Palaeouplift only found oil and gas display but no shale
72 industrial gas flow (Xie et al., 2014), demonstrating the gas diversity of Niutitang
73 formation on the periphery of Sichuan Basin Outer palaeouplift. Taking four typical
74 wells around the palaeouplift as analysis objects, based on the analysis of shale gas
75 geological conditions, the research focuses on analyzing and discussing the
76 influencing factors and main controlling factors that affect the gas content of shale gas
77 on the periphery of the ancient uplift, in order to find favorable areas for Niutitang
78 shale gas exploration in the outer Sichuan Basin and serve a new round of oil and gas
79 prospecting breakthrough.

80 2. Geological setting and sampling sections

81 The Cambrian shales in south China generally have a high degree of thermal
82 evolution, and the study area is located in the eastern and northern margins of Sichuan
83 Basin, from north to south are respectively Hannan Palaeouplift, Shenlongjia
84 Palaeouplift, Huangling Palaeouplift and Xuefengshan Palaeouplift. The paleouplift
85 experienced tectonic uplift in the Paleozoic, and its rigid basement structure was
86 stable, which was conducive to shale gas preservation. For the southern Cambrian
87 ancient formations, the paleouplift has early uplifting time and short deep burial time,
88 and the thermal evolution of the Cambrian shale is lower than that of other regions.

89 Seven wells on the periphery of four ancient uplifts were selected as the research
90 objects, including Well 1 and Well 2 on the southern margin of Hannan Ancient Uplift,
91 Well 3 on the western margin of Shenlongjia Ancient Uplift, Well 4 on the southwest
92 margin of Huangling Ancient Uplift and Well 5 on the southeast margin of Huangling
93 Ancient Uplift, Well 6 and Well 7 on the southwest margin of Xuefengshan Ancient
94 Uplift (Fig.1).

95 **3. Samples and analytical methods**

96 **3.1. Samples**

97 In this study, data were collected from 7 wells in the paleouplift, including 35
98 samples from Well 1, 25 samples from Well 2, 18 samples from Well 3, 120 samples
99 from Well 4, 50 samples from Well 5, 49 samples from Well 6, and 12 samples from
100 Well 7. Detail information of studied wells are listed in Table 1.

101 **3.2 Experimental methods**

102 In this study, seven wells from four palaeouplifts were selected to carry out
103 organic geochemical experiments, such as TOC, Asphalt reflectance, organic matter
104 types, etc. Reservoir physical properties, such as rock and mineral composition,
105 porosity, permeability, pore type, fracture development, etc. Gas content testing
106 experiments, such as field Desorption gas content measurement, gas component
107 analysis, isothermal adsorption, etc. In addition, the well logging data, hydrocarbon
108 generation history and structural evolution history in the study area were studied.

109 The experiments of organic geochemistry and reservoir physical properties were
110 determined by the Geochemical Laboratory of Yangtze University. Since the sample

111 comes from the old formation of Niutitang Formation, the sample does not contain
112 vitrinite, which cannot be measured by conventional vitrinite reflectance. The bitumen
113 reflectance was measured and converted to Ro. The gas content and gas composition
114 were determined by YSQ-IV analytical analyzer, which was independently developed.
115 During the determination process, continuous drainage gas collection method was
116 applied to collect gas samples and analyze gas composition. The desorption gas and
117 residual gas were directly measured by this method, and the total gas content was
118 finally calculated by combining with the simulation of lost gas.

119 **4. Results**

120 **4.1. Organic geochemical characteristics**

121 The research area consists of seven wells that are deposited in the continental
122 shelf to slope facies. The dominant organic matter type is Type I, with high organic
123 carbon content. These wells are located on the periphery of an ancient uplift.
124 According to the theory "Reservoir control at the margin of paleo-uplift" (Zhai et al.,
125 2017). Compared with southeast Chongqing area and West Hunan and Hubei area, the
126 degree of thermal evolution in the study area is relatively low, which is the main
127 consideration for drilling.

128 The kerogen type of Well 1 is type I, and the organic carbon content is 0.52% -
129 3.02%, with an average of 1.5%. TOC of the lower and middle parts with good gas
130 content can reach more than 2.0%. The maturity of organic matter is high, and the
131 results of Ro range from 2.48% to 4.36%, with an average of 3.0%, which is in the
132 stage of over-mature evolution. TOC content of 31 core samples from Well 2 ranges

133 from 0.88% to 8.61%, with an average value of 3.37%. The shale with TOC_{>2%} has a
134 thickness of 78m, and the maturity of 34 samples ranges from 2.04% to 3.14%, with
135 an average value of 2.66%, and is in the over-mature cracking gas stage. The main
136 types of organic matter are type I and type II₁ (Xu et al., 2019).

137 The TOC of Well 3 Niutitang Formation is between 0.49% - 4.14%, with an
138 average of 1.96%, and the vitrinite reflectance Ro is between 3.02% and 3.25%,
139 which has entered the mature evolution stage, and the maceral of kerogen is
140 dominated by sapropelic amorphous type. TOC of the Niutitang Formation of Well 4
141 ranges from 0.04%-3.88% with an average of 2.01%, and the lower part of the second
142 segment of Niutitang Formation with a better gas content ranges from 0.68%-3.88%
143 with an average of 2.44%. The vitrinite reflectance Ro is between 2.0% and 2.77%,
144 which entered the mature to overmature stage. The TOC of the gas-bearing shale of
145 Well 5 Niutitang Formation ranges from 0.43% - 10.45% with an average of 2.62%,
146 and the TOC of the shale of 1832 m - 1872 m ranges from 1.23% - 10.45% with an
147 average of 3.45%. The maceral of kerogen is mainly sapropelic amorphous type,
148 organic matter type I, Ro ranges from 2.06% - 2.66% with an average of 2.29%,
149 which is in the stage of over-mature evolution.

150 The abundance of organic matter in Niutitang Formation in the South Guizhou
151 Depression is generally high (Teng et al., 2008). The TOC of Niutitang Formation in
152 Well 6 ranges from 0.60% to 8.89%, with an average of 3.55%. Ro ranges from
153 1.43% to 2.81%, with an average of 2.37%, which belongs to the early stage of
154 maturation and overmaturity. The main kerogen was type I, and a small amount was

155 type II 1. In addition, 30 stable carbon isotope experiments of kerogen show that δ
156 $^{13}\text{C}_{\text{org}}$ ranges from -29.2‰ to -34.7‰, indicating that it is type I kerogen. The TOC
157 of Niutitang Formation in Well 7 is 0.25% - 8.72%, with an average of 3.56%. R_o has
158 the characteristics of upper and lower height, the distribution range is 3.26% - 4.4%,
159 the average is 3.9%, and it is in the late over-mature - metamorphic stage, especially
160 after the bottom 997 m, R_o is greater than 4%, and it is in the metamorphic stage. The
161 organic matter type is mainly type I (Table 2).

162 **4.2. Reservoir property**

163 The brittle mineral content of core samples from Well 1 Niutitang Formation
164 ranges from 52.7% to 74.1%, mainly quartz. The main clay minerals are chlorite,
165 kaolin-ite, illite and montmorillonite. The measured porosity ranges from 0.02% to
166 5.17%, with an average value of 2.01% by Overburden pore permeability test. The
167 porosity measured by mercury injection ~~experiment~~ was 1.7% - 2.78%, with an
168 average value of 2.15%. The permeability ranges from 0.00053 mD to 0.0041 mD,
169 with an average value of 0.0008 mD, which belongs to the low porosity ultra-low
170 permeability reservoir. The pores can be divided into three categories: mineral matrix
171 pores, organic matter pores and micro-fractures, among which micro- fractures are
172 mainly marginal cracks between organic matter and inorganic minerals, with a slit
173 width of 0.5 μm - 8.6 μm (Wang, 2014). The brittle mineral content of Niutitang
174 Formation in Well 2 ranges from 40.6% to 64.8%, with an average of 53.6%, among
175 which quartz content is the highest, ranging from 47% to 25.6%, with an average
176 content of 37.16%. The pore types are mainly mineral dissolution pores,

177 intercrystalline pores of pyrite are occasionally found, and organic pores are few.
178 Microfractures are abundant, and the seam width is 0.5 μ m -8.6 μ m (Wang et al.,
179 2014).

180 The brittle mineral content of Niutitang Formation in Well 3 is the highest 74%,
181 and the average is 50%. The porosity is 1.45%-8.04%, with an average of 3.33%, and
182 the permeability is 0.0005 mD -0.004 mD, with an average of 0.0015 mD. The pore
183 types include intergranular pores, intra-granular pores, organic pores, solution pores,
184 mold holes and micro-fractures. The fractures are mainly high Angle fractures with
185 large dip Angle and low density. Some fractures have crossover phenomenon and are
186 mostly filled with calcite.

187 There are differences in mineral composition among different formations in Well
188 4 Niutitang Formation. The lower part of the second segment of Niutitang Formation,
189 which has the best gas content and the highest organic matter abundance. It is
190 dominated by quartz with an average content of 37%, followed by carbonate rock,
191 clay (illite and chlorite), the average content of 19%, the pyrite content is relatively
192 high, up to 3% on average. Other segment are dominated by calcite. The porosity
193 ranges from 2.01% to 3.61%, with an average value of 2.88%. Permeability ranges
194 from 0.00031 mD to 0.00078 mD with an average of 0.00054mD. The pores are rich
195 in organic matter, followed by the solution pores and micro-fractures, which is a low
196 porosity and ultra-low permeability reservoir. A total of 34 (half) filling cracks and 66
197 open cracks were picked up from the electrical imaging data. The dip Angle of the
198 opening seam is between 20.3 and 89.7, and the inclination is mainly south. The

199 fracture trajectory is clear, indicating that the fracture has good connectivity and
200 ductility (Liu et al., 2019) (Fig. 2).

201 The brittle mineral content of Well 5 is high, ranging from 45% to 75%, shale
202 gas-bearing interval from 1788 m to 1872 m, in which the content of carbonate and
203 clay minerals is higher in the shale from 1788 m to 1832 m, and the content of quartz
204 minerals is lower. The mineral content in the smaller depth section changes greatly,
205 and the material composition is obviously heterogeneous. The content of quartz and
206 clay minerals is high and the content of carbonate minerals is low in the shale of 1
207 832 m -1 872 m, and the mineral content changes relatively little in the shale of small
208 depth, and the rock mineral composition is relatively stable. The reservoir space is
209 divided into three types: inorganic pore, organic pore and microfracture.
210 Microfractures are mainly layered fractures inside clay minerals, which have good
211 extensibility and connectivity, and can optimize the transformation of pore system (Li
212 et al., 2003).

213 The brittle mineral content of Well 6 is high, ranging from 37% to 68%, with an
214 average of 51%. The quartz content is 28%-53%, with an average of 37.8%. The
215 average porosity and permeability of Niutitang Formation are 0.51% and 0.001mD
216 respectively. The microcosmic reservoir space is dominated by matrix pores, followed
217 by organic pores. Pyrite is common and a few residual pores can be seen. The
218 fractures are mainly manifested as tensile cracks and slip cracks. Affected by the
219 detachment structure, it is mainly filled with calcite veins. The above two groups of
220 fractures have the characteristics of multi-phase, staggered with each other, and local

221 grid shape.

222 The content of quartz minerals in Niutitang Formation of Well 7 is 35.1% -
223 51.8%, with an average of 43.5%. The brittle mineral is high, which is conducive to
224 the later fracturing. The upper part of Niutitang Formation has an average porosity of
225 2%, which corresponds to high gas content. The reservoir space is dominated by
226 inorganic mineral matrix pores, with micro-fractures and undeveloped organic pores.
227 Micropores are connected with microfractures, forming a complex network of pores
228 and fractures with good connectivity (Diaz et al., 2013). More high-angle fractures are
229 often filled with quartz, calcite, pyrite and other minerals, and the filling degree is
230 relatively high.

231 **4.3. Gas-bearing**

232 The highest total hydrocarbon in Well 1 Niutitang Formation 2201.00m-2271.00m
233 and 2353.00m-2387.00m is 4.28%. The Desorption gas content is 0.2 m³/t -4.5m³ /t, in
234 which the gas content is greater than 2 m³/t between 2150 m and 2380m. The total gas
235 content of Well 2 is 0.77 m³/t -3.39m³/t, showing high gas content. The gas content
236 increases gradually with the depth.

237 The overall gas content of Well 3 is low, and the maximum gas content is 0.13m³/t
238 in the 1156.62m - 1852.76m. At the top of Niutitang Formation, 1454 m - 1591m, a gas
239 anomaly occurred, with a maximum total hydrocarbon value of 3.65%.

240 The Desorption gas content of Well 4 is 0.13m³ / t- 2.16m³ /t, and the total gas
241 content is 0.26m³ / t- 4.48m³ /t, among which 2980 m - 3055m has a higher gas content
242 with an average of 2.3m³/t. The core bubbles violently ~~in water immersion test~~, and the
243 ~~gas ignition~~ is flammable. The test shows that the daily gas production is 7.83×10⁴ m³
244 /d, and the open flow rate is 28.84×10⁴m³ / d. The gas content of Well 5 is 0.58 m³ /t -

245 5.48m³/t. Among them, the gas content of the well depth of 1837 m - 1872m is greater
246 than 2 m³/t, and the average is 2.78 m³/t; the gas content of the well depth of 1854 m -
247 1872m is greater than 3 m³/t, and the average is as high as 3.8 m³/t. The daily gas
248 production is 6.02×10⁴m³/d and the open flow is 12.38×10⁴m³/d.

249 The Desorption gas content in Well 6 ranges from 0.09 m³/t to 1.11m³/t, with an
250 average value of 0.42 m³/t. The total gas content of upper well samples is relatively
251 high. The gas content of Niutitang Formation in Well 7 ranges from 0.06 m³/t - 1.97m³/t
252 with an average of 0.32m³/t. There are two high gas content segments in the middle and
253 upper part. The first segment is 957 m - 975m with calcareous carbonaceous shale and
254 the maximum gas content is 1.1m³/t. Second, in the 1005m - 1013m segment, gas
255 penetration occurred at the wellhead during drilling, and the maximum gas content was
256 1.97m³/t. The gas logging showed a high gas anomaly with a maximum value of 7.92%
257 (Fig. 3).

258 5. Discussion

259 Previous studies on the geological conditions of shale gas formation on the
260 periphery of palaeouplift put forward a new shale gas enrichment model in the slope
261 belt of palaeouplift margin, which is "favorable facies zone is the foundation, organic
262 matter content is the guarantee, basement uplift and evolution is the key", and guided
263 the breakthrough of shale gas exploration. However, the Niutitang shale, which is also
264 located in the periphery of the ancient uplift in the outer Sichuan Basin, still has great
265 differences in gas-bearing properties. By analyzing the relationship between degree of
266 thermal evolution, structural preservation condition, sedimentary subfacies, reservoir
267 physical property and gas-bearing, the main controlling factors of gas-bearing in shale
268 surrounding different palaeouplift are studied.

269 5.1. Analysis of rich gas conditions

270 (1) Correlation between gas content and maturity

271 On the basis of the study of 7 wells in this paper, 9 wells in the adjacent area are
272 investigated and analyzed comprehensively (Fig. 4)—. Based on the relationship
273 between Ro and gas content of 16 wells, it is found that: 1). The correlation between Ro
274 and gas content is weak and linear, and the correlation coefficient is 0.47. 2). The value
275 of Ro can qualitatively reflect the size of the gas content. ① As can be seen from the
276 figure, there are 8 data with Ro higher than 3%, and the Ro value is 3.06% - 3.40%,
277 with an average of 3.20%. The gas content is 0.13 m³/t - 1.2m³/t, the average is 0.75
278 m³/t, and the gas content of 50% data is less than 1 m³/t. ② There were 7 data whose
279 Ro value was less than or equal to 3%, with a value of 2.15% - 2.95% and an average of
280 2.57%. The gas content is 1.38 m³/t - 3.00m³/t, with an average of 2.19 m³/t, and the gas
281 content of 71% data is greater than 2 m³/t. The average Ro of the three wells obtained
282 shale gas flow is 2.40%, and the gas content is 2.13 m³/t - 3.00m³/t, with an average of
283 2.67 m³/t. Therefore, the degree of thermal evolution is the key factor affecting gas
284 content. The Ro of well 6 is 2.37% and the gas content is low. The reason is that the gas
285 content of well 6 is not only affected by Ro, but also restricted by other factors.

286 (2) Differential tectonic subsidence affects the degree of thermal evolution

287 Although the seven wells are located in the periphery of the outer palaeouplift of
288 Sichuan Basin, the differences of thermal evolution degree and hydrocarbon generation
289 are caused by different tectonic subsidence in different regions. Compared with
290 Huangling Palaeouplift and Xuefeng Palaeouplift, Ro in Wells 4 and 5 is generally
291 lower than 3.0%, while the minimum Ro in 7 wells are higher than 3.0%. The main
292 reasons are as follows:

293 First, the deep burial time is late, the deep burial time is short, the thermal
294 evolution degree is low, and it is in the best gas generation period, which is beneficial to

295 gas content. The Niutitang Formation shale of Huangling Uplift entered the
296 oil-generating stage in the middle Silurian, entered the thermal cracking condensate
297 oil-gas stage at the end of Permian, and remained relatively stable until the middle
298 Triassic. At present, the shale Ro of Niutitang Formation in Well 4 and Well 5 is
299 2.26%-2.77%, and the latter is smaller with an average of 2.29%, which is in the best
300 gas window range. From the end of Permian to the beginning of Triassic, it experienced
301 rapid subsidence, and was in the deep burial period (>3500m) in the late Jurassic
302 (before Yanshan uplift), with a deep burial time of about 85Ma (Fig.5). The
303 hydrocarbon generation time of Niutitang Formation in Well 7 was early. The
304 Niujutang Formation was buried rapidly after deposition, and entered the hydrocarbon
305 generation threshold in the early Middle Cambrian (about 508 Ma), the burial depth
306 exceeded 3500 m in the Late Cambrian, reached the late oil-generation and early gas
307 generation stage until the early Middle Triassic (before the Indo uplift), and was in the
308 continuous deep gas burial stage with the maximum burial depth exceeding 5700m and
309 the hydrocarbon generation time exceeding 270Ma. Deep burial time (>3500m)
310 exceeds 250Ma (Fig. 6). It can be seen that the southern margin of Huangling Uplift is
311 generally shorter than that of Niutitang Formation on the western margin of Xuefeng
312 uplift (Nie et al., 2021) and the deep burial time is later, resulting in a lower degree of
313 thermal evolution and still in the optimal gas generation stage, which is more conducive
314 to shale gas enrichment.

315 Second, hydrothermal intrusion along the fault may lead to an increase in the
316 degree of thermal evolution. The comparison of Ro% between Well 7 Doushantuo
317 Formation and Niutitang Formation shows that the Ro% of Doushantuo Formation is
318 3.32%-3.59%, but it is significantly lower than the lower part of Niutitang Formation. It
319 is believed that the small fault drilled at the bottom of Niutitang may locally warm the

320 shale in Niutitang, resulting in abnormal maturity, while the Doushantuo shale is
321 normal geothermal warming, which is lower than the maturity of the lower part of
322 Niutitang Formation. The main reasons are as follows: ① the first member of
323 Niutitang Formation consists of gray-black thin-layer siliceous rocks,
324 phosphorus-bearing siliceous rocks and phosphorite nodules with thickness of 2 m
325 -15m. This phosphorus may be related to the volcano, and there may be volcanic
326 hydrothermal intrusion, which increases the temperature of Niutitang Formation. (2)
327 The fault was drilled at the bottom of Niutitang Formation, which penetrated the
328 Dengying Formation, and hydrothermal minerals such as barite, fluorite and quartz
329 were found in the cracks. From this point of view, it is very likely that the hydrothermal
330 migration of Dengying Formation along the fault affected the temperature of Niutitang
331 Formation and accelerated the thermal evolution of organic matter.

332 **5.2. The relationship between structural preservation and gas-bearing**

333 (1) Major Faults characteristics

334 Fracture is closely related to shale gas-bearing and mainly controls the
335 preservation conditions of shale gas. Faults can be used not only as a migration
336 pathway of shale gas to cause gas loss and damage shale gas preservation (Gao et al.,
337 2014), but also as a shale gas sealing formation to prevent gas loss and facilitate shale
338 gas enrichment (Hu et al., 2014). It can even be used as a release pathway of tectonic
339 energy to control the integrity of the formation. Therefore, by analyzing the fractures
340 and their properties of different research objects, the influence of fractures on shale
341 gas preservation can be comprehensively judged.

342 The fault structure of Qinling region in southern Shaanxi is complex, and in

343 addition to some regional plate edge faults and intra-plate faults, there are also buried
344 faults (Zhang et al., 2004). Under the influence of late Indosinian and Yanshanian
345 strong uplift, the Micangshan tectonic belt is a forward-spreading structure from north
346 to south caused by the superposition of two thrust nappe structures in different
347 directions. From the initial underwater uplift, it rose to land after the Indochina
348 movement. Among them, Well 1 is mainly affected by the Yangpingguan-Yangxian
349 fault in the near east-west direction, while Well 2 is surrounded by the
350 Dachimba-Zhenba fault in the near east-west direction and the Sishang-Xiaoyangba
351 fault in the north-west-southeast direction (Chen et al., 2018).

352 There is a regional fault-Yangriwan Fault on the western margin of Shennongjia
353 (He et al., 2021). And Well 3 is located about 1km to the south of the fault. Several
354 fracture zones and a buried fault were found during drilling. The core of the dark
355 shale section has different degrees of fractures and is partially or completely filled
356 with calcite.

357 There are fault structures of different periods, different scales and different
358 directions in western Hubei, which form a regular network. Some important faults
359 constitute the division boundary of the secondary tectonic units, and have obvious
360 control over the regional structural styles, and are also of great significance to the
361 preservation of shale gas. Well 4 and 5 are located on the Yichang slope, with the
362 Wuduhe fault in the southeast, which breaks into the core of the uplift and serves as
363 the boundary of the stable region of the southern Yichang slope belt together with the
364 Tianyangping fault (Fig.7).

365 The eastern part of the Qiannan Depression is bounded by the Tonren-Sandu
366 fault and the Xuedeng Uplift (Bai et al., 2010); the southeast part is bounded by the
367 Libo Fault and the Guizhong Depression; the southwest part is bounded by the
368 Ziyun-Luodian-Nandan -Du 'an fault and the Luodian Fault depression; the northwest
369 part is bounded by the Guiyang-Zhenyuan fault and the Qianzhong Uplift, and the
370 plane is a triangle that is wide in north and narrow in south. It mainly presents three
371 groups of fault systems with different scales in the NNE - near SN, NW, NEE - near
372 EW direction (Peng et al., 2019).

373 (2) The relationship between structural preservation and gas-bearing
374 Well 4 and 5 are located in the bottom of thrust nappe, with relatively stable,
375 simple structure and few faults, which is conducive to the preservation of shale gas. The
376 Niutang Formation of Well 1 is deformed by long-term compression, with deep gully,
377 broken terrain and strong dynamic geological action, which is not conducive to shale
378 gas preservation. Well 4, located about 1km south of the major fault, encountered
379 several fracture zones and a buried fault during drilling. The core of the dark shale
380 section has varying degrees of fractures, and is partially or completely filled with
381 calcite. The mirror scratches can be seen in the natural section of the core of the two
382 wells 1824.06m-1824.12m, which indicates that the tectonic movement in this area is
383 relatively intense, which is not conducive to the preservation of shale gas.

384 Although Well 6 and Well 7 are located in the Qiannan Depression, Well 7 is
385 located in the Danzhai area, which is far from the fault position, the formation of
386 Niutang Formation is stable, and the degree of structural deformation is relatively
387 weak (Dan et al., 2023). However, there are three regional large faults around Well 6,
388 and a number of secondary small faults develop near the well. Due to the relatively

389 staggered formation, the low-grade tension-torsion fault develops in the direction of
390 65° NW, making the Huangping fault zone more complicated and damaging the
391 preservation conditions (Ge et al., 2018; 2020), resulting in slightly lower gas content
392 in Well 6 than Well 7. In addition, there are many faults in the south Guizhou
393 Depression with multi-stage and complex structure, and the gas components can reflect
394 the destructive effect of faults on the gas content of shale. The nitrogen content of Well
395 7 is 30%, while the nitrogen content of Well 6 is 50-79%, indicating that the gas
396 contains atmospheric components. Considering that the gas-bearing formation is
397 connected with the atmosphere through fracture, the enrichment of shale gas is
398 destroyed. The higher atmospheric content in Well 6 also confirms that the gas
399 reservoir is more destructive and has relatively lower gas content.

400 In addition, the fracture is favorable to the gas content of shale gas. The Niutitang
401 Formation, where Well 4 and 5 are located, is located in the footwall of thrust nappe
402 and has a stable structure. It plays an effective role in releasing stress during multi-stage
403 structural transformation, thus protecting the upper overlying Sinian, Cambrian, Upper
404 Ordovician and Lower Silurian shales from being strongly damaged on the rigid base.
405 From the perspective of integrity and stability of source rock development, fracture has
406 a favorable influence on shale enrichment.

407 **5.3. The relationship between sedimentary subphase and gas-bearing**

408 Favorable sedimentary facies zones control the hydrocarbon generation capacity
409 of source rocks, are the material basis of shale gas enrichment, and are closely related to
410 gas-bearing properties. From the successful development examples and experiences of
411 shale gas in Wufeng-Longmaxi Formation in China (Guo et al., 2014), it can be seen
412 that deep-water facies deposits such as deep-water shelf are one of the most important
413 theories in the “ternary enrichment model” theory of shale gas (Guo et al., 2014). The

414 favorable facies zone model of the Carboniferous platform basin-lower slope facies in
415 the south of Guizhou and the middle of Guangxi has guided the shale gas investigation.

416 (1) Sedimentary characteristics

417 The sedimentary environment determines the material basis of shale gas
418 formation. ~~The division scheme of sedimentary environment of Niutitang Formation~~
419 ~~in the four palaeouplifts in the study area can be divided into two categories: The first~~
420 ~~type is classified as shelf facies, which can be subdivided into two subfacies: deep~~
421 ~~shelf and shallow shelf, which is adopted by most scholars. The second category is~~
422 ~~divided into rifting trough facies, which can be subdivided into aulacogen basin and~~
423 ~~slope subfacies (Zhai et al., 2017).~~

424 In general, southern Shaanxi belongs to passive continental margin deposits on
425 the northern margin of the Upper Yangtze Block. According to the first classification
426 scheme, the Niutitang Formation of Well 1 and Well 2 in southern Shaanxi is mainly
427 shallow shelf sedimentary subfacies, and the high-quality shale segment is deep shelf
428 subfacies. The better gas-bearing member of the two wells is the middle and lower
429 part of Niutitang Formation, and the lithology is dark gray carbonaceous shale, silty
430 shale, silty carbonaceous shale with carbonaceous siltstone and marl. According to the
431 second category, Well 1 is the slope subfacies, and Well 2 is the aulacogen basin
432 facies of the rift trough.

433 The Niutitang Formation in Shennongjia area is mainly composed of
434 sedimentary shelf facies and slope facies, among which shelf facies can be further
435 divided into deep water shelf subfacies ~~and shallow water shelf subfacies~~, and slope

436 facies can be divided into slope foot subfacies (Xie et al., 2017). The Niutitang
437 Formation can be divided into the first, second and third members from the bottom up,
438 corresponding to deep shelf subfacies, shallow shelf subfacies and slope foot
439 subfacies respectively. The first segment of Niutitang Formation with ~~better~~
440 ~~gas-bearing~~ is characterized by deep grayish-black calc-carbonaceous mudstone,
441 black calc-carbonaceous mudstone, argillaceous siltstone lamination, rich pyrite
442 nodules and pyrite bands. According to the second classification, the sedimentary
443 environment is rifted trough basin subfacies.

444 Tectonic evolution controls the distribution of sedimentary facies zones in
445 Yi-chang area of western Hubei. In the early Cambrian, influenced by the large-scale
446 transgression of the Yangtze River, the sediments in this area were successively
447 composed of tidal flat facies, shallow water facies and deep shelf facies from
448 northeast to southwest (Zhang et al., 2023). Both Well 4 and 5 are deepwater shelf
449 facies, and the former has deeper water. The second segment of Niutitang Formation,
450 lithology of which is gray-black and black carbonaceous shale, is a deep water shelf
451 deposit. According to the second classification, Well 4 is aulacogen basin and Well 5
452 is slope subfacies (Fig. 8).

453 The paleogeothermal environment of Niutitang Formation in the Qiannan
454 Depression has low water temperature and dark anoxic deposits, and the organic
455 matter is well preserved. The sedimentary environment of Well 6 and 7 is deep shelf -
456 subdeep sea basin deposition. The second member of Niutitang Formation with good
457 gas-bearing capacity is gray-black mudstone, mixed with gray argillaceous limestone,
458 containing pyrite nodules or bands. A complete trilobite fossil was found in Niutitang

459 Formation in Well 6. According to the second classification, Well 6 is aulacogen basin,
460 and Well 7 is deep shelf deposition.

461 (2) The relationship between sedimentary subphase and gas-bearing
462 The Niutitang Formation in the study area has the characteristics of multi-stage
463 hydrocarbon generation of organic matter. The results show that the Niutitang
464 Formation generally has the characteristics of high organic matter abundance, and the
465 influence of organic matter abundance is usually ignored when analyzing the
466 influencing factors of shale gas content in the Niutitang Formation. According to the
467 analysis of sedimentary facies of 7 wells, all of them belong to rifting trough facies.
468 However, in the case of similar thermal evolution degree and structural preservation
469 conditions, although Hannan palaeouplift and Huangling palaeouplift belong to the
470 same sedimentary zone - West Hubei Trough, due to different sedimentary subfacies,
471 the hydrocarbon generation capacity of shale is affected, and thus the gas content of
472 shale is affected(Fig.9). Although Well 1, 2 and 4 are all located in the same large
473 rifting trough, and the thermal evolution degree of the key factor for the Niutitang
474 Formation is generally less than 3.0%, different sedimentary subfacies lead to
475 differences in their gas-bearing properties. Well 2 and 4 are subfacies of rifting trough
476 basin, while Well 1 is subfacies of rifting trough slope. The sedimentary environment is
477 different, which leads to the lower hydrocarbon generation potential of shale in Well 1
478 than that in Well 2 and 4, resulting in the difference of gas content. In addition, the
479 stable gas flow of $21 \times 10^4 \text{ m}^3/\text{d}$ in Well Shanzhenye 1 in Zhenba area, which is adjacent
480 to Well 2, also confirms the controlling effect of sedimentary subfacies relative gas
481 content.

482 5. Conclusions

483 (1) Hydrocarbon control by sedimentation. The main reason that the gas content

484 of Well 1 is lower than that of Well 2 is that the former is slope facies of rifting trough
485 and the latter is deep water facies of rifting trough basin. The difference of
486 hydrocarbon generation potential caused by sedimentary subfacies in the same facies
487 zone is an important factor restricting the gas content of shale.

488 (2) Thermal ~~evolution degree~~ control zone. The rigid basement on the periphery
489 of the ancient uplift has the effect of "heat insulation and preservation", which makes
490 the ~~thermal evolution degree~~ of the periphery generally low, and most of them have
491 not entered the graphitization stage. However, the differences in the thermal evolution
492 degree of the Niutitang shale on the periphery of different ancient uplift due to the
493 deep burial starting time, deep burial time span and deep burial rate are the key factors
494 restricting the gas content of the shale.

495 (3) Preservation control the reservoir. As a relatively stable area of the Niutitang
496 Formation around the ancient uplift, the difference in preservation conditions caused
497 by the structural strength, fracture development degree and the coupling relationship
498 with tectonic fractures is the key factor restricting the gas- bearing of shale

499 (4) The geological conditions of shale gas enrichment at the periphery of
500 palaeouplift, favorable preservation conditions such as lower plate of thrust nappe,
501 moderate thermal evolution degree and deep water facies area of trough are favorable
502 directions for further exploration.

503 **Acknowledgments**

504 We sincerely thank Prof. Zhai for his sedimentary facies figures that greatly
505 improved the manuscript. This work was supported by the National Natural Science

506 Foundation of China (42130803) and the Geological Survey Project (DD20230257).

507

In review

508 **References:**

- 509 HAMMES, U., FRBOURG, G, 2012. Haynesville and Bossier mudrocks: a facies and sequence stratigraphic
510 investigation, East Texas and Louisiana, USA. *Marine and Petroleum Geology* 31, 8-26.
- 511 Abouelresh, M.O., Slatt, R.M., 2012. Lithofacies and Sequence Stratigraphy of the Barnett Shale in EastCentral
512 Fort Worth Basin, Texas. *AAPG Bulletin* 96, 1-22.
- 513 Bruner, K.R., Walker-Milani, M., Smosna, R., 2015. Lithofacies of the Devonian Marcellus Shale in the Eastern
514 Appalachian Basin, U.S. A. *Journal of Sedimentary Research* 85, 937-954.
- 515 He, Z.-L., Nie, H.-K., Zhang, Y.-Y., 2016. Analysis of the main controlling factors of shale gas enrichment in the
516 Ordovician Wufeng Formation and Silurian Longmaxi Formation in Sichuan Basin and its peripheral areas.
517 *Earth Science Frontiers* 23, 8-17.
- 518 He, Z.-L., Nie, H.-K., Li, S.-J., Liu, G.-X., Ding, J.-H., Bian, R.-K., Lu, Z.-Y., 2021. Differential occurrence of
519 shale gas in the Permian Longtan Formation of Upper Yangtze region constrained by plate tectonics in the
520 Tethyan domain. *Oil & Gas Geology* 42, 1-15.
- 521 Bao, S.-J., Zhai, G.-Y., Zhou, Z., Yu, S.-F., Chen, K., Wang, Y.-F., Wang, H., Liu, Y.-M., 2018. The evolution of the
522 Huangling uplift and its control on the accumulation and preservation of shale gas. *China Geology* 1,
523 346-353.
- 524 Li, H., Liu, A., Luo, S.-Y., Chen, X.-H., Chen, L., 2019. Characteristics of the Cambrian Shuijingtuo shale
525 reservoir on Yichang Slope, western Hubei Province: a case study of well EYY 1. *Petroleum Geology &
526 Experiment* 41, 76-82.
- 527 Zhang, J.-F., Zhai, G.-Y., Wang, D.-M., Bao, S.-J., Chen, K., Li, H.-H., Song, T., Wang, P., Zhou, Z., 2020. Tectonic
528 evolution of the Huangling dome and its control effect on shale gas preservation in the north margin of the
529 Yangtze Block, South China. *China Geology* 3, 28-37.

530 Xie, Z., Lu, S.-F., Yu, L., Chen, Y.-P., Wang, M., Chen, F.-W., He, X.-P., 2014. Assessment of Natural Gas Loss
531 from Mudstone Gas Source Rocks — an Example from Jiumenchong Formation of Huangye 1 Well, Lower
532 Cambrian, Southern Guizhou Sag, China. *Acta Mineralogica Sinica* 34, 137-143.

533 Xie, X.-N., Hao, F., Lu, Y.-C., He, S., Shi, W.-Z., Jiang, Z.-X., Xiong, Y.-Q., Zhang, J.-C., 2017. Differential
534 Enrichment Mechanism and Key Technology of Shale Gas in Complex Areas of South China. *Earth Science*
535 42, 1045-1056.

536 Zhang, Y., Huang, D.-J., Zhang, L.-L., Wan, C.-H., Luo, H., Shao, D.-Y., Meng, K., Yan, J.-P., Zhang, T.-W., 2023.
537 Biogenic silica of the Lower Cambrian Shuijingtuo Formation in Yichang, western Hubei Province—features
538 and influence on shale gas accumulation. *Earth Science Frontiers* 30, 83-100.

539 Gao, J., He, S., He, Z.-L., Zhou, Y., Zhao, M.-L., 2014. Genesis of Calcite Vein and Its Implication to Petroleum
540 Preservation in Jingshan Region, Mid-Yangtze. *Oil&Gas Geology* 35, 33-41.

541 Hu, D.-F., Zhang, H.-R., Ni, K., Yu, G.-C., 2014. Main Controlling Factors for Gas Preservation Conditions of
542 Marine Shales in Southeastern Margins of the Sichuan Basin. *Natural Gas Industry* 34, 17-23.

543 Zhang, G.-W., Dong, Y.-P., Lai, S.-C., Guo, A.-L., Meng, Q.-R., Liu, S.-F., Cheng, S.-Y., Yao, A.-P., Zhang, Z.-Q.,
544 Pei, X.-Z., 2004. Mianlue tectonic zone and Mianlue suture zone at the southern margin of the Qinling-Dabie
545 orogenic belt. *Science China: Earth Sciences* 47, 300-316.

546 Chen, X.-L., Zhai, G.-Y., Bao, S.-J., Pang, F., Wang, J.-Z., Tong, C.-C., 2018. Shale gas accumulation and
547 gas-bearing properties of Niutitang formation in well Zhendi 1, Zhenba region of southern Shaanxi province.
548 *China Mining Magazine* 27, 101-106.

549 He, W., Chen, Y., Lei, Y.-Y., Qian, C., Chen, K., Lin, T., Song, T., 2021. Analyses of the relationship between
550 lithology and shale gas accumulation for the Wufeng Formation to Longmaxi Formation in the west of Hubei
551 Province: A case study of the Erhongdi 1 well. *Journal of China Coal Society* 46, 1014-1023.

552 Bai, Y.-S., Xiong, C.-Y., Wang, C.-S., Li, X.-B., Liu, A., Zhang, M., 2010. Tectonic Evolution of North Area of
553 Xuefengshan Uplift and Its Relation to Marine Hydrocarbon Formation. *Geology and Mineral Resources of*
554 *South China* 96, 68-75.

555 Peng, Z.-Q., Tian, W., Miao, F.-B., Wang, B.-Z., Wang, C.-S., 2019. Geological Features and Favorable Area
556 Prediction of Shale Gas in Lower Cambrian Niutitang Formation of Xuefeng Ancient Uplift and Its Periphery.
557 *Earth Science* 44, 3512-3528.

558 Zhai, G.-Y., Bao, S.-J., Wang, Y.-F., Chen, K., Wang, S.-J., Zhou, Z., Song, T., Li, H.-H., 2017. Reservoir
559 Accumulation Model at the Edge of Palaeohigh and Significant Discovery of Shale Gas in Yichang
560 Area, Hubei Province. *Acta Geoscientica Sinica* 38, 441-447.

561 Xu, T., Xu, F., Guo, Y.-H., Wang, N., Xie, Q.-Z., Huang, W., 2019. Organic geochemical characteristics of the
562 Lower Paleozoic shales in Xixiang-Zhenba Area, Southern Shaanxi. *Journal of Northeast Petroleum*
563 *University* 43, 59-68.

564 Teng, G.-E., Qin, J.-Z., Zheng, L.-Y., 2008. Hydrocarbon Potential on Excellent Hydrocarbon Source Rock in
565 Southern Guizhou Depression and Its Spatial-Temporal Distribution. *Acta Geologica Sinica* 82, 366-372.

566 Wang, Y.-M., Dong, D.-Z., Yang, H., He, L., Wang, S.-Q., Huang, J.-L., Pu, B.-L., Wang, S.-F., 2014. Quantitative
567 characterization of reservoir space in the Lower Silurian Longmaxi shale, southern Sichuan, China. *Science*
568 *China(Earth Sciences)* 57, 313-322.

569 Liu, L., He, S., Zhai, G.-Y., Chen, K., Liu, Z.-X., Wang, Y., Han, Y.-J., Dong, T., 2019. Diagenetic Environment
570 Evolution of Fracture Veins of Shale Core in Second Member of Niutitang Formation in Southern Limb of
571 Huangling Anticline and Its Connection with Shale Gas Preservation. *Earth Science* 44, 3583-3597.

572 Lee, S.G., Lee, D.H., Kim, Y., Chae, B.G., Woo, N.C., 2003. Rare Earth Elements as Indicators of Groundwater
573 Environment Changes in a Fractured Rock System: Evidence from Fracture-Filling Calcite. *Applied*

574 Geochemistry 18, 135-143.

575 Diaz, H.G., Lewis, R., Miller, C., Fuentes, C.C., 2013. Evaluating the Impact of Mineralogy on Reservoir Quality
576 and Completion Quality of Organic Shale Plays. AAPG Rocky Mountain Section Meeting, Salt Lake City,
577 USA.

578 Nie, G-Q., Li, X.-P., Dan, Y., Liang, B., Zhang, Q.-Y, Li, J.-R., Ji, S.-C., 2021. Burial and thermal history of mud
579 shale in Niutitang formation of lower Cambrian in southern Guizhou depression:A case study of Guidudi well
580 1. Carsologica Sinica 40, 760-767.

581 Dan, Y., Yan, J.-F., Bao, S.-J., Lang, B., Ma, L., Nie, G-Q., Cao, J.-F., Ji, S.-C., Han, K., 2023. Discovery of
582 Sinian-Cambrian multi-tier shale gas in Guidandi-1 well of southwest margin of Xuefeng uplift. Geology in
583 China 50, 291-292.

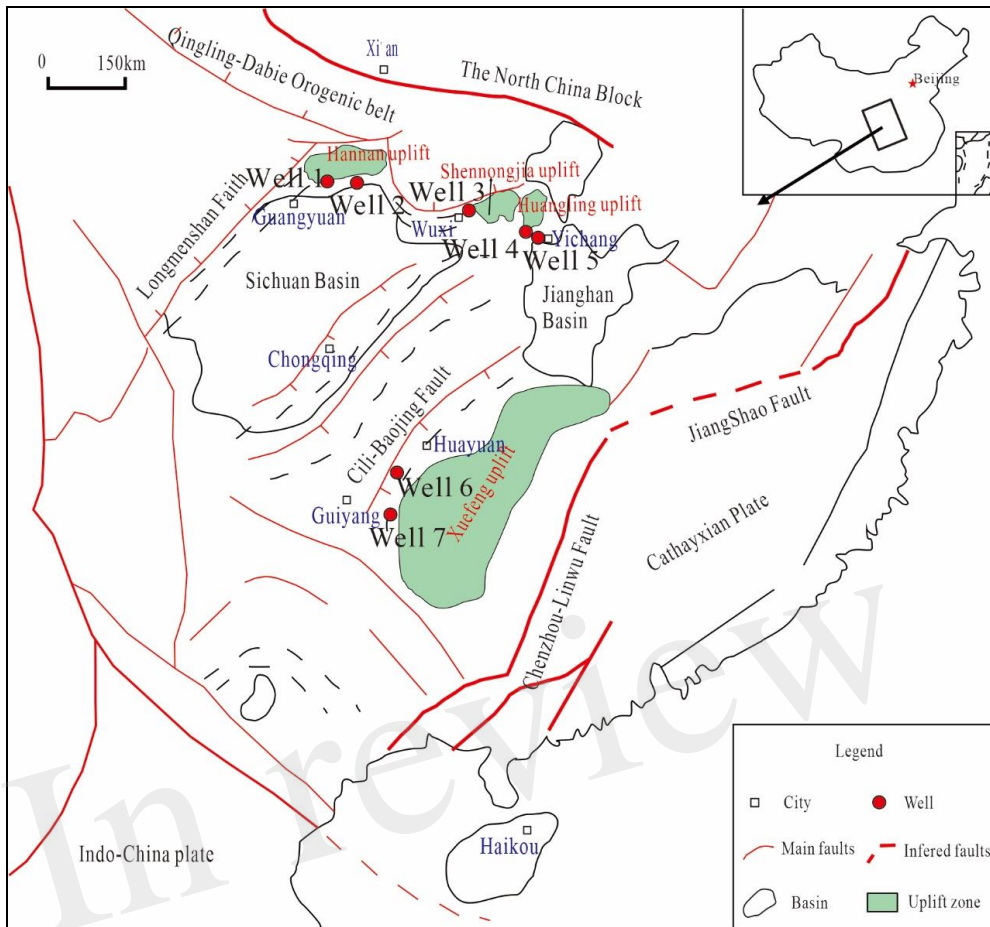
584 Ge, M.-N., Chen, K., Chen, X.-L., Wang, C., Bao, S.-J., 2020. The influence factors of gas-bearing and geological
585 characteristics of Niutitang Formation shale in the southern margin of Xuefeng Mountain ancient uplift: A
586 case of Well Huangdi 1. Geology in China 3, 533-544.

587 Ge, M.-N., Bao, S.-J., He, W., Chen, X.-L., Lin, T., Chen, K., 2018. The discovery of shale gas in Lower Cambrian
588 marine shale gas at Huangdi-1 Well in Huangping region of northern Guizhou. Geology in China 45, 851-852.

589 Guo, X.-S., 2014. Rules of Two-Factor Enrichment for Marine Shale Gas in Southern China——Understanding
590 from the Longmaxi Formation Shale Gas in Sichuan Basin and Its Surrounding Area. Acta Geologica Sinica
591 88, 1209-1218.

592 Guo, T.-L., Zhang, H.-R., 2014. Formation and enrichment mode of Jiaoshiba shale gas field,Sichuan Basin.
593 Petroleum Exploration and Development 41, 28-36.

594



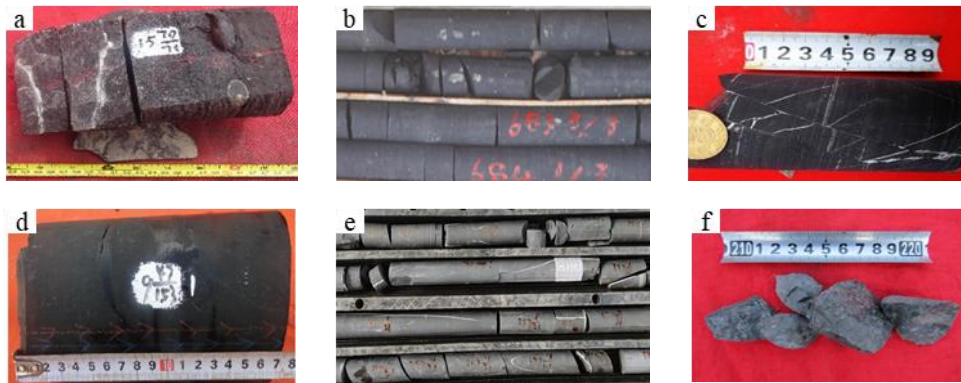
596

597 Fig.1. Study area and drilling structure location.

598 Well 1 and 2 belong to the periphery of Hannan Palaeohigh, Well 3 belong to the periphery of
 599 Shennongjia Palaeohigh, Well 4 and 5 belong to the periphery of Huangling Palaeohigh, and
 600 Well 6 and 7 belong to the periphery of Xuefeng Palaeohigh.

601

602



603 Fig.2 Core fractures of Niutitang Formation in different drilling wells.

604 (a) Core fracture of Niutitang Formation in Well 1, along with bedding fracture, are partially filled;

605 (b) The core fracture of Niutitang Formation in Well 2, along with the bedding joint, is not filled;

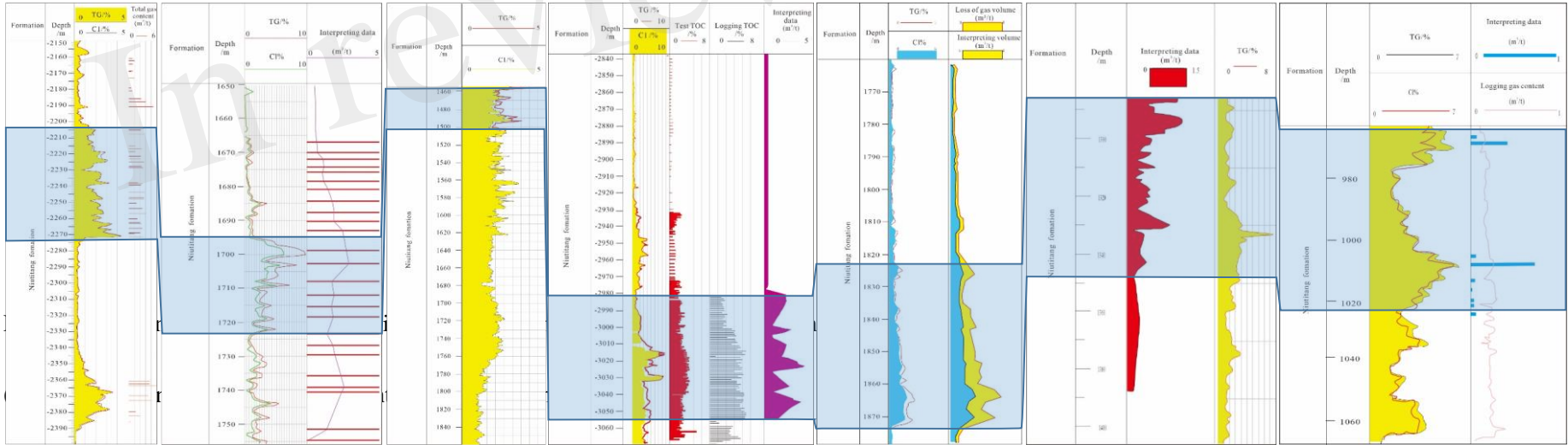
606 (c) The cracks of Niutitang Formation in Well 3 are filled with calcite, and the filling degree is

607 high; (d) The core crack of Niutitang Formation in Well 4 is open and not filled; (e) Niutitang

608 Formation of Well 6 has high Angle shear fracture and high filling degree; (f) Core fracture of

609 Niutitang Formation, Well 7, Slip cracks, core breakage.

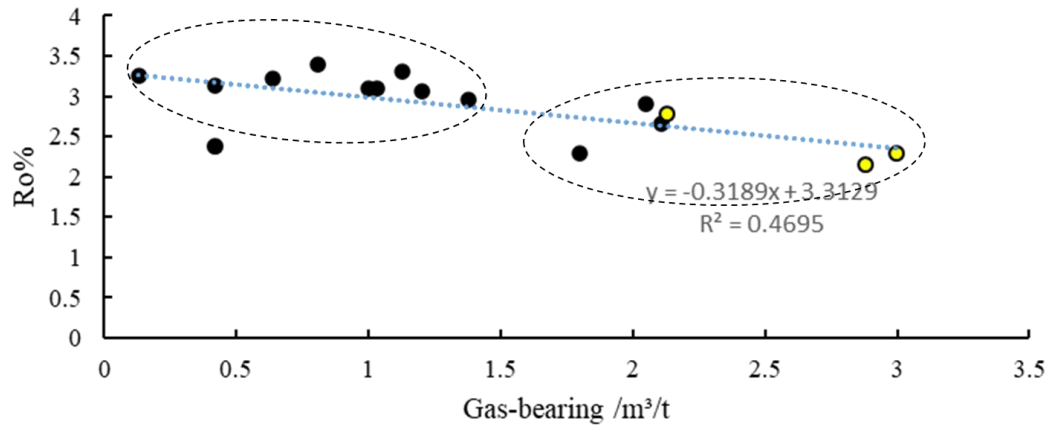
610



611

612

613

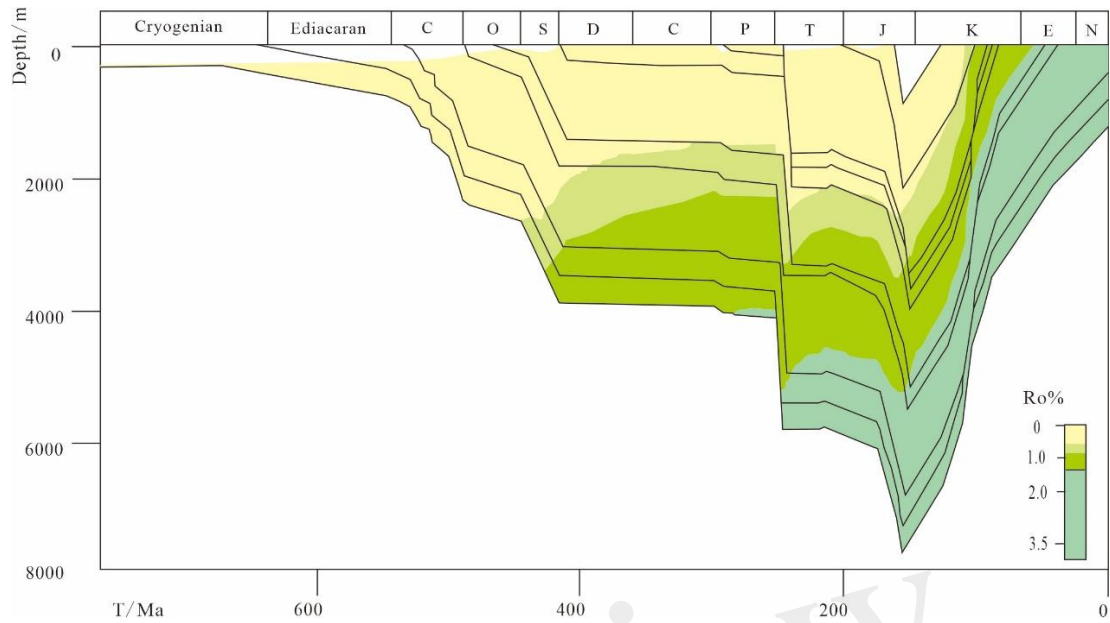


614

615 Fig.4 Relationship between Ro and gas content

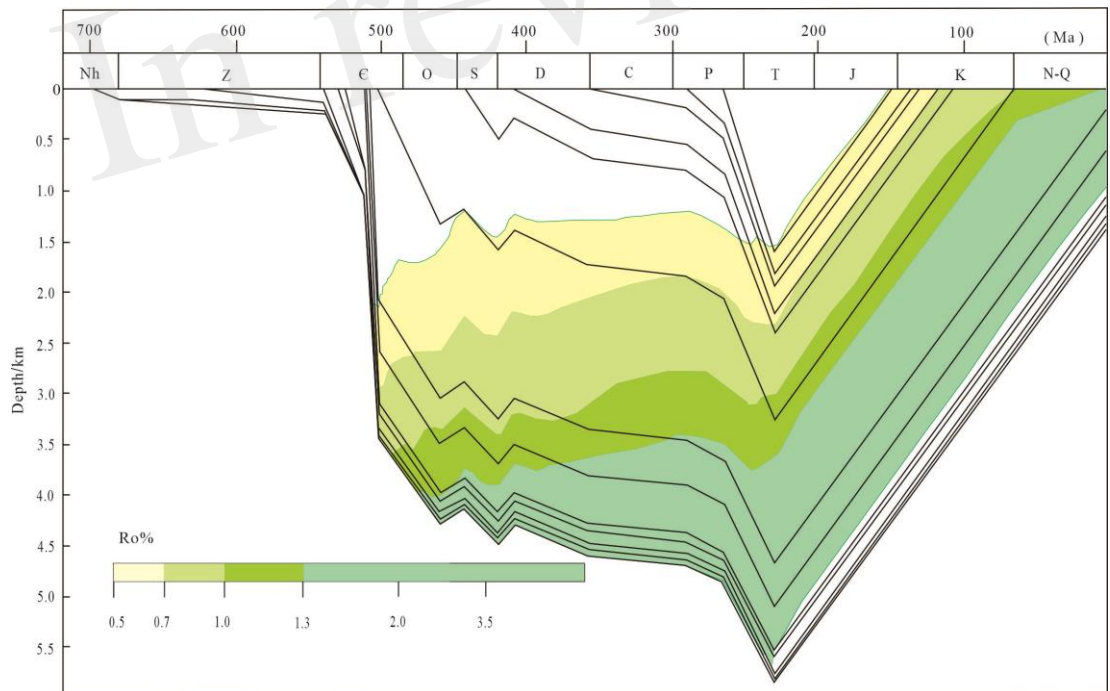
In review

616



617

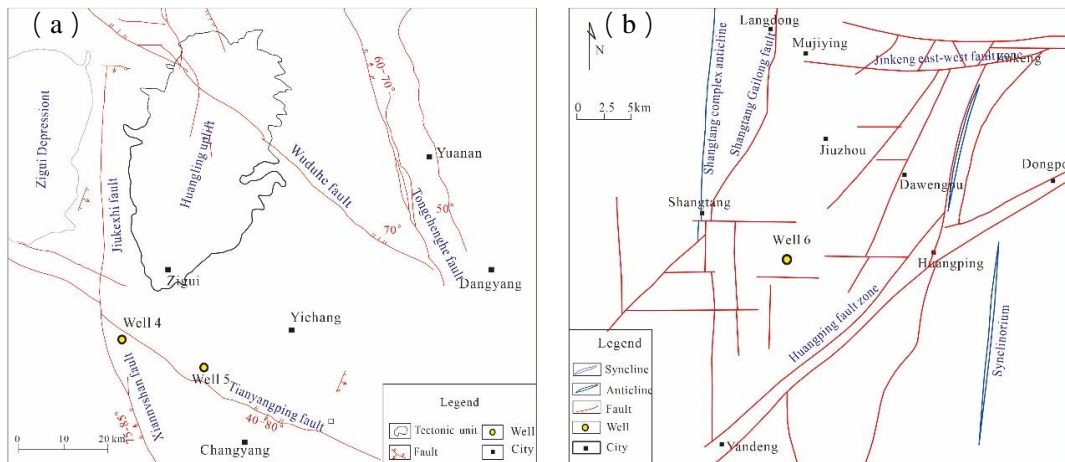
618 Fig.5 History of sedimentary burial in Huangling palaeouplift



619

620 Fig.6 History of sedimentary burial in Xuefeng palaeouplift

621

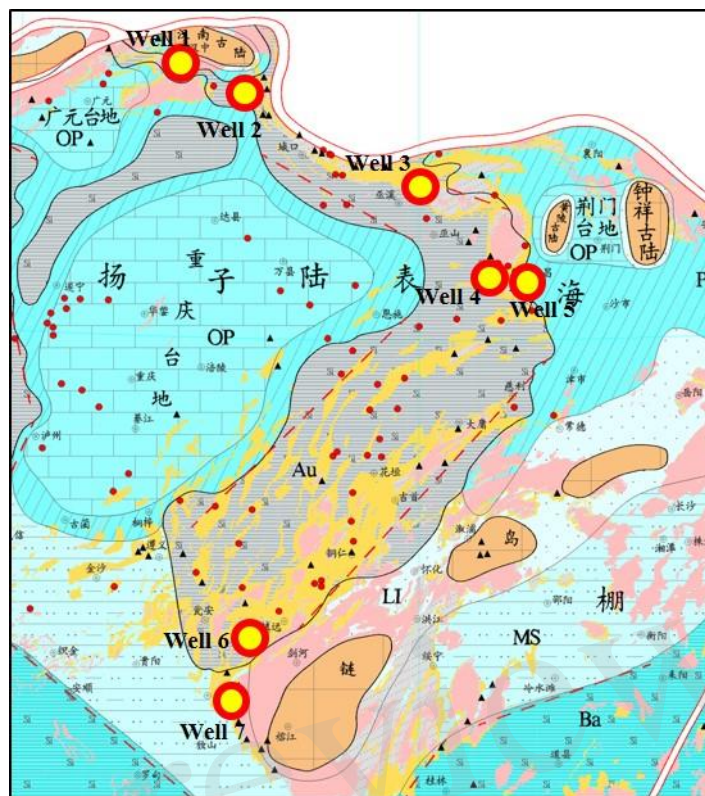


622 Fig.7 Distribution of major faults.

623 (a) periphery of Huangling Uplift. (b) periphery of Xuefeng Uplift.

624

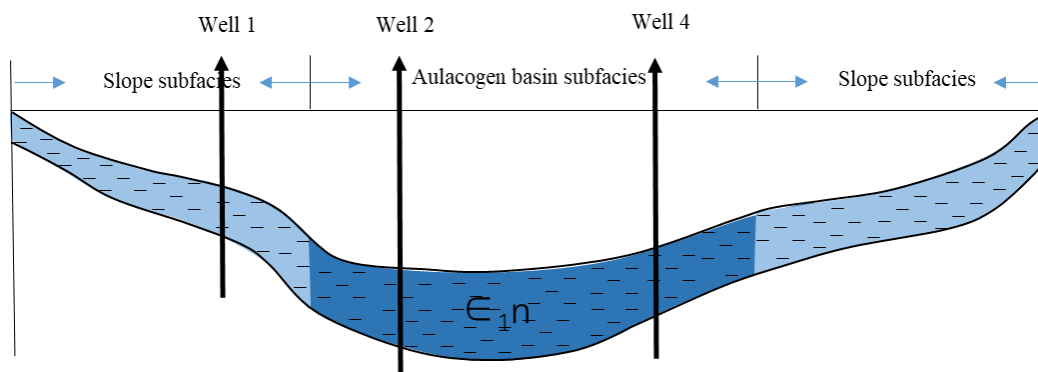
In review



626

627 Fig.8 Sedimentary facies of Niutitang Formation in the study area (modified by Zhai Gangyi)

628



629

630 Fig.9 Schematic diagram in the Aulacogen basin sedimentary subfacies of Niutitang formation

631

In review

632 **Tables:**

633 Table 1 Information of 7 wells

Well number	Geographical position	Tectonic position	Well type	Formation	Depth m	Start drilling formation	Completed formation	Hydrocarbon indication
1	Nanzheng, Shaanxi	Between Hannan Uplift and Micang Mountain uplift	Parameter well	Niutitang Formation	2150-2380	Permian	Nanhuan (Nantuo Formation)	Gas showing
2	Zhenba, Shaanxi	Southeastern margin of Micang Mountain uplift	Survey well	Niutitang Formation	1670-1750	Silurian	Sinian (Dengying Formation)	gas show strong
3	Shennongjia, Hubei	Northern wing of Shennongjia complex anticline	Survey well	Niutitang Formation	1454-1852	Silurian	Sinian (Dengying Formation)	No gas show
4	Changyang, Hubei	South margin of Huangling uplift	Parameter well	Niutitang Formation	2600-3069	Cambrian	Nanhuan (Nantuo Formation)	Industrial gas flow
5	Dianjun, Hubei Province	South margin of Huangling uplift	Parameter well	Niutitang Formation	1787-1871	Cretaceous	Nanhuan (Nantuo Formation)	Industrial gas flow
6	Huangping, Guizhou	Southwest margin of Xuefeng uplift	Survey well	Niutitang Formation	1286-1406	Cambrian	Nanhuan (Nantuo Formation)	Gas showing
7	Danzhai, Guizhou	Southwest margin of Xuefeng uplift	Survey well	Niutitang Formation	960-1070	Cambrian	Sinian (Doushantuo Formation)	Gas showing

634

635 Table 2 Basic geological parameters of 7 wells

Well number	Fault/structure	Lithology	Thickness /m	TOC /%	R ₀ /%	Gas content m ³ /t	Production *10 ⁴ /d	Brittle mineral /%	Porosity /%	permeability /mD	Fracture
1	Less/ weak deformation	Black carbonaceous shale	103.5	0.52-3.02/1.5	2.48-4.36/3.0	0.2-4.4	inproductivity	52.7-74.1	0.02-5.17/2.01	0.00053-0.0041/0.0008	rich
2	Less/ weak deformation	Dark grey siliceous carbonaceous shale interspersed with carbonaceous siltstone	90	0.88-8.61/3.37	2.04-3.14/2.66	0.77-3.39	inproductivity	40.6-64.8/53.6	/	/	rich
3	Many/ strong structure	Gray-black calcareous silty mudstone interbedded with argillaceous limestone	397.86	0.49-4.14/1.96	3.02-3.25	0.0002-0.13/0.032	inproductivity	20-74/50	1.45-8.04/3.33	0.0005-0.004/0.0015	are mostly filled
4	Less/Structural stability	Shale, mixed with argillaceous limestone and argillaceous siltstone	468.5	0.04-3.88/2.01	2.0-2.77	0.26-4.48	7.83	55-75	2.01-3.61/2.88	0.00031-0.00078/0.00054	rich
5	Less/Structural stability and simple	Gray-black gray shale with dark gray argillaceous limestone	86	0.43-10.45/2.62	2.06-2.66/2.29	0.58-5.48	6.02	45-75	1.48-2.5	/	rich
6	Many/ Strong structure	Black carbonaceous shale	119.95	0.60-8.89/3.55	1.43-2.81/2.37	0.09~1.31/0.42	inproductivity	37~68/51	0.2 ~ 1.8/0.51	0.0001-0.01/0.001	Slip fracture
7	Many/ Strong structure	Black carbonaceous mudstone	105	0.25-8.72/3.55	3.26-4.4	0.06~1.97	inproductivity	35.1-51.8/43.5	0.65-1.21	0.001-0.012	are mostly filled

636 Note: "/" represents the average value.

Figure 1.JPEG

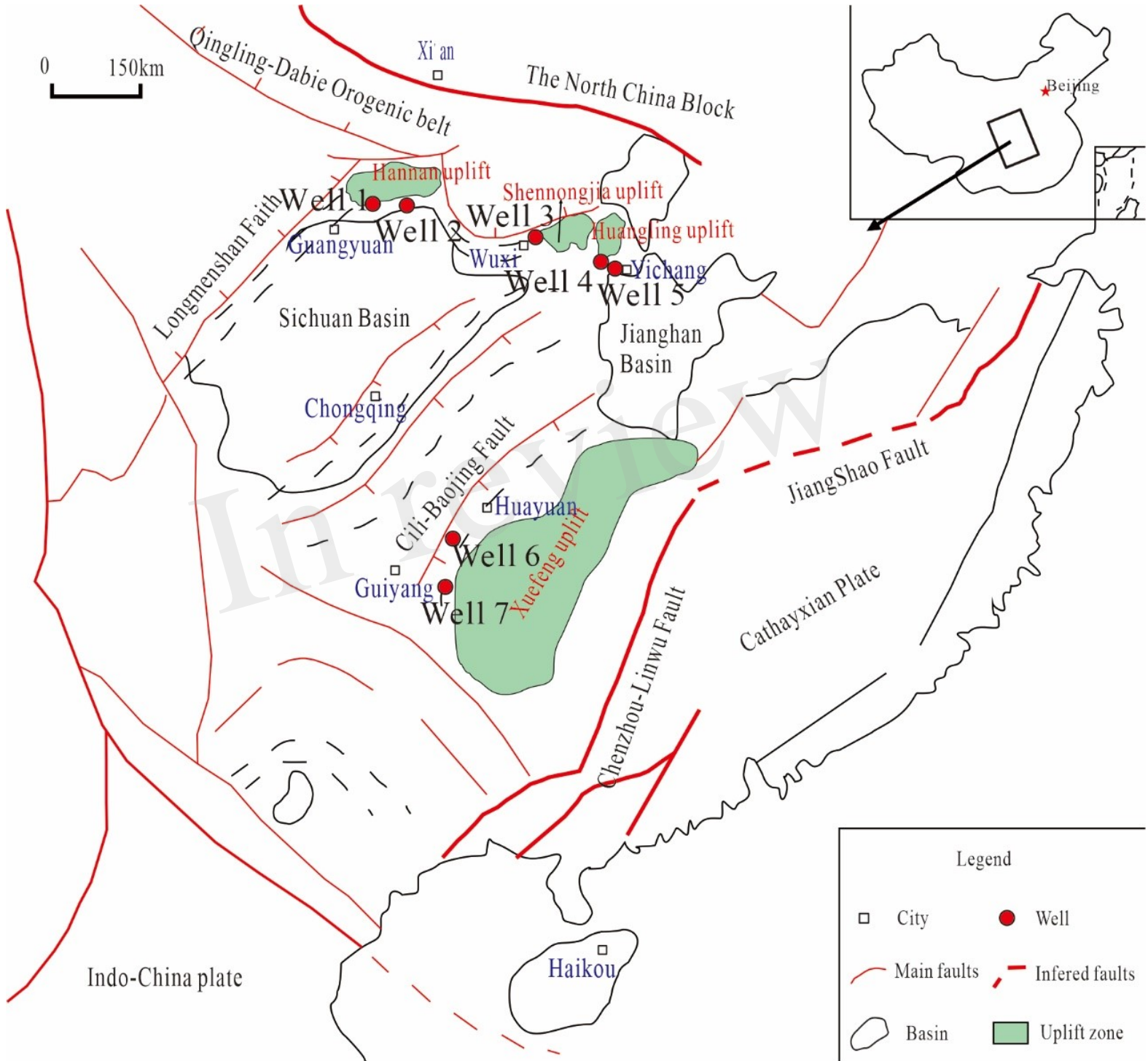


Figure 2.JPEG

In review



Figure 3.JPEG

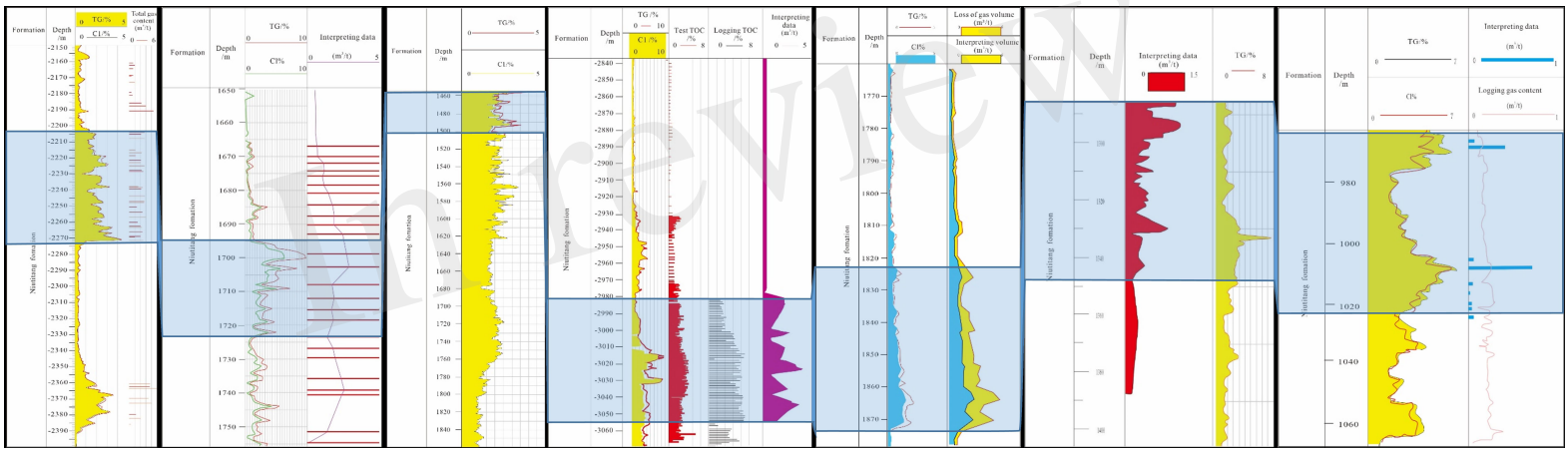


Figure 4.JPEG

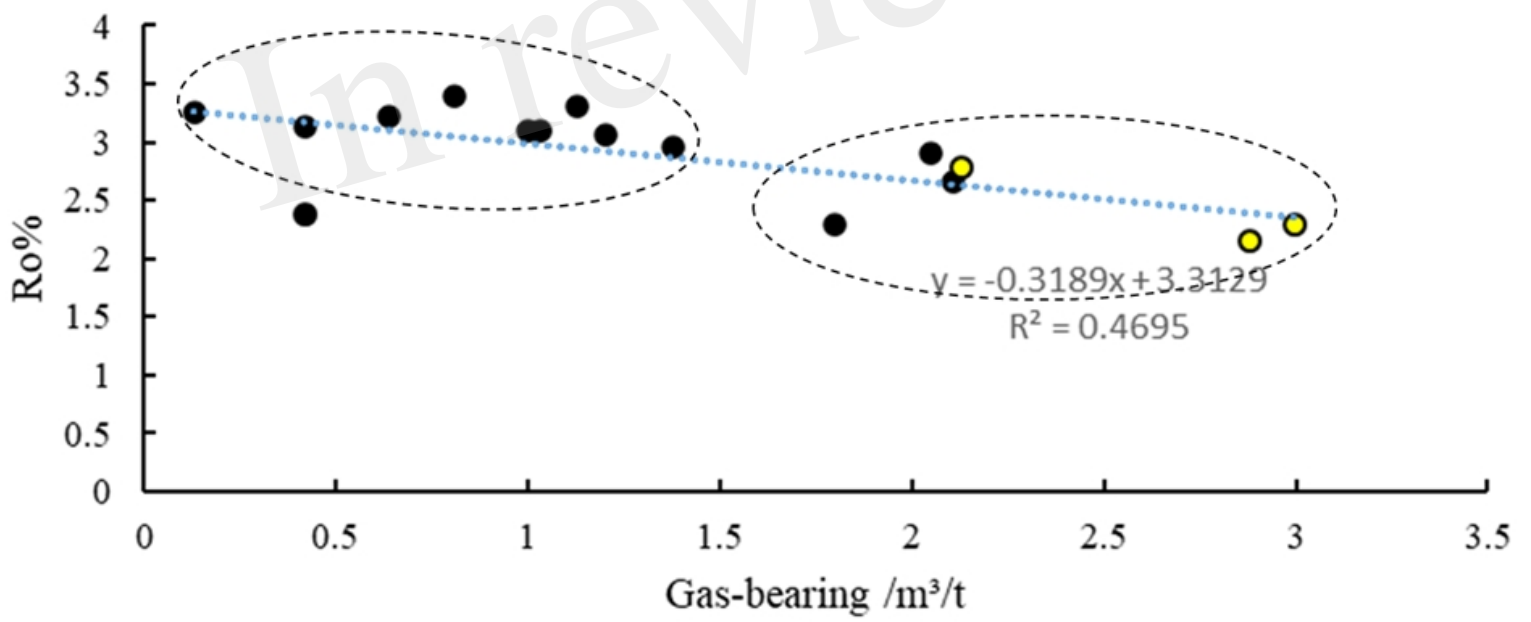


Figure 5.JPEG

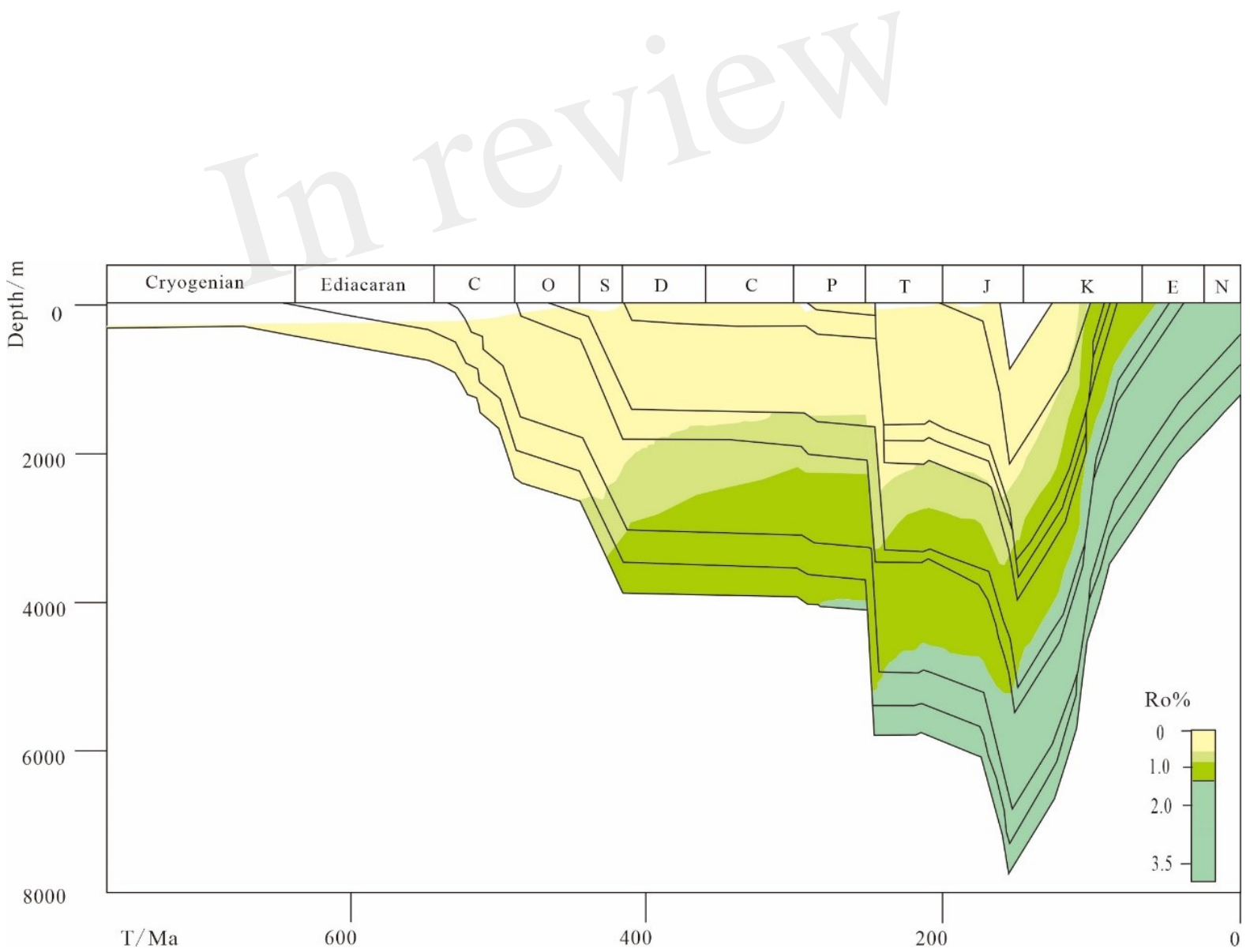


Figure 6.JPEG

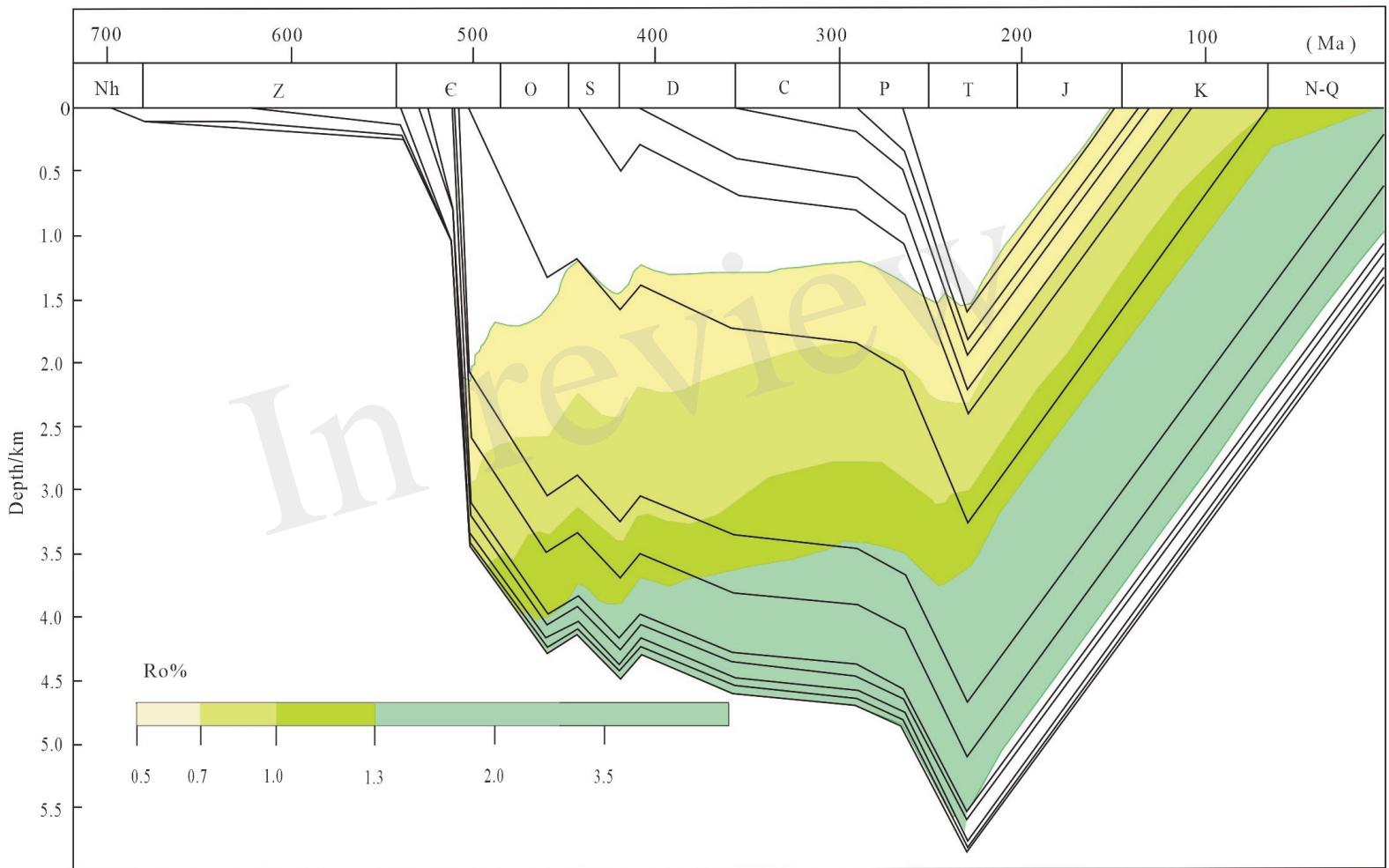


Figure 7.JPEG

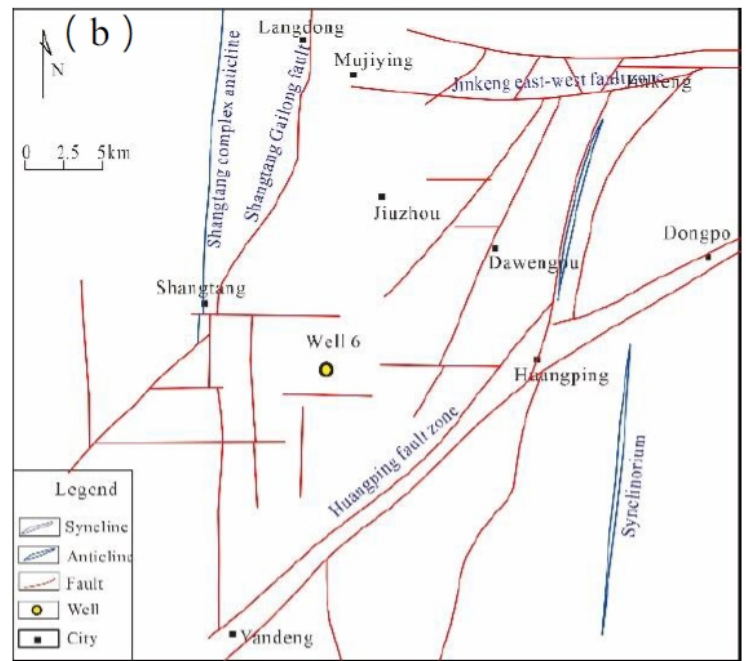
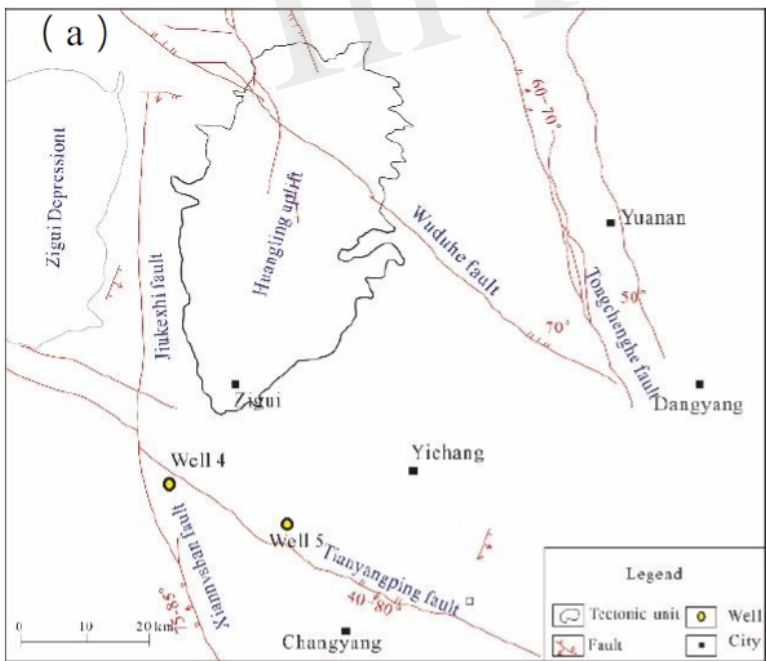


Figure 8.JPEG

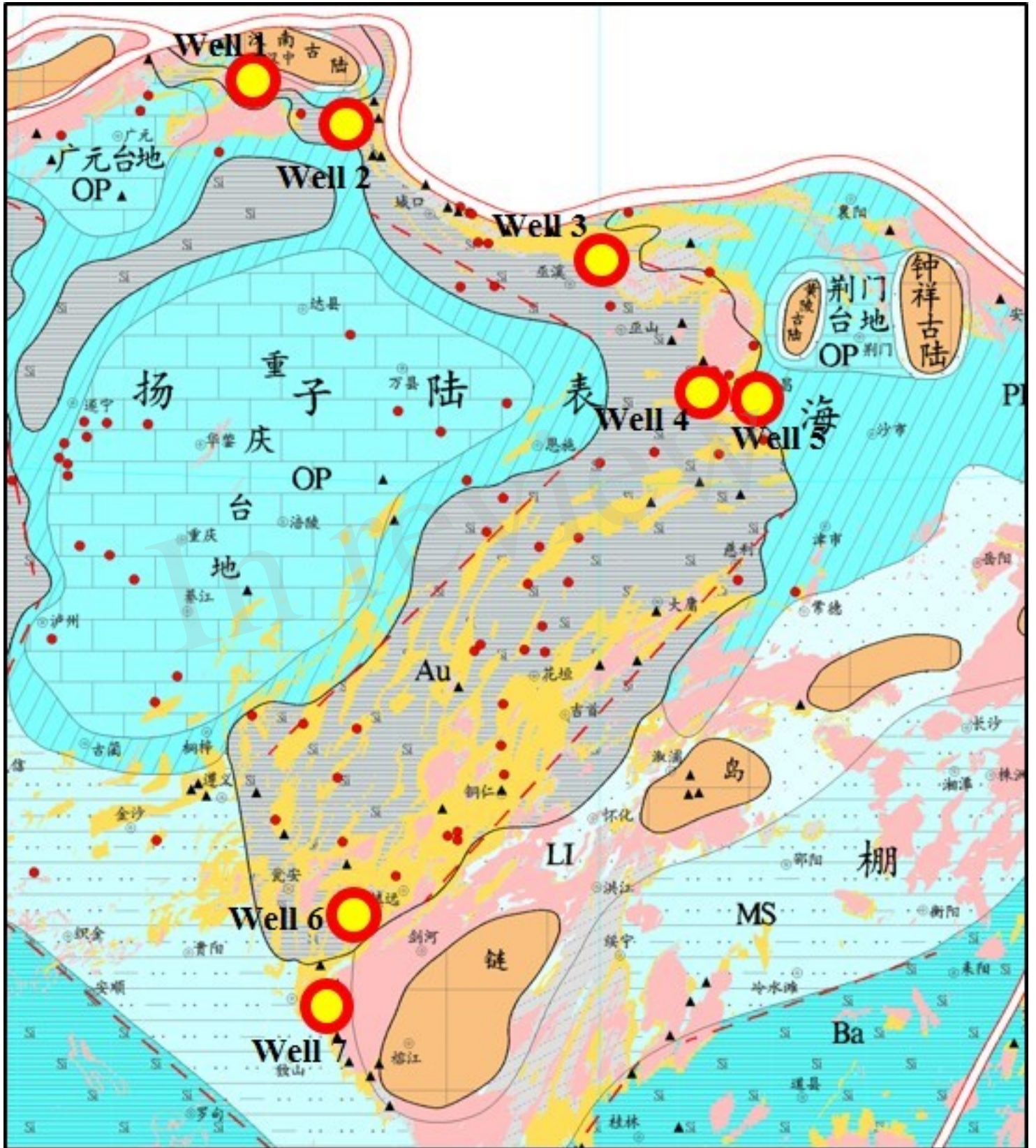


Figure 9.JPG

